COMPLEX SYSTEM MODELING AND SIMULATION
ISSN 2096-9929 06/06 pp 145–161
Volume 1, Number 2, June 2021
DOI: 10.23919/CSMS.2021.0011

Multi-Robot Indoor Environment Map Building Based on Multi-Stage Optimization Method

Hui Lu, Siyi Yang, Meng Zhao, and Shi Cheng*

Abstract: For a multi-robot system, the accurate global map building based on a local map obtained by a single robot is an essential issue. The map building process is always divided into three stages: single-robot map acquisition, multi-robot map transmission, and multi-robot map merging. Based on the different stages of map building, this paper proposes a multi-stage optimization (MSO) method to improve the accuracy of the global map. In the map acquisition stage, we windowed the map based on the position of the robot to obtain the local map. Furthermore, we adopted the extended Kalman filter (EKF) to improve the positioning accuracy, thereby enhancing the accuracy of the map acquisition by the single robot. In the map transmission stage, considering the robustness of the multi-robot system in the real environment, we designed a dynamic self-organized communication topology (DSCT) based on the master and slave sketch to ensure the efficiency and accuracy of map transferring. In the map merging stage, multi-layer information filtering (MLIF) was investigated to increase the accuracy of the global map. We performed simulation experiments on the Gazebo platform and compared the result of the proposed method with that of classic map building methods. In addition, the practicability of this method has been verified on the Turtlebot3 burger robot. Experimental results proved that the MSO method improves the accuracy of the global map built by the multi-robot system.

Key words: multi-robot system; map merging; multi-robot communication; swarm intelligence

1 Introduction

Compared with the single-robot system, the multi-robot system has higher working efficiency, better task completion efficiency, lower production cost, and other advantages[1]. The multi-robot system has been applied in different environments in a multitude of fields. In particular, the indoor environment is one of the popular environments for multi-robot applications that have received extensive attention[2–7]. The cooperation of the robots in an indoor environment relies on a consistent and reliable global map[8]. Therefore, map building is one of the important challenges faced by the multi-robot system. An efficient and accurate map-building mechanism is of great significance to the multi-robot system.

Considering the application of the multi-robot system in the real environment, the multi-robot map building technology faces many challenges. First, the accuracy of the global map is based on the mapping ability of the single robot. Therefore, the impact of the positioning error of a single robot should be considered in the map building process. Second, a lot of researches in the field of map building have only focused on obtaining a

• Hui Lu, Siyi Yang, and Meng Zhao are with the School of Electronic and Information Engineering, Beihang University, Beijing 100191, China. E-mail: mluhui@buaa.edu.cn; siyiyang0215@foxmail.com; meng960416@163.com.
• Shi Cheng is with the School of Computer Science, Shaanxi Normal University, Xi'an 710119, China. E-mail: cheng@snnu.edu.cn.
∗ To whom correspondence should be addressed.
Manuscript received: 2021-04-26; revised: 2021-05-11; accepted: 2021-05-21

high-precision global map while ignoring the efficiency of map building[9]. In addition, the robustness of the system is not considered during the map transmission process, and one or more faulty robots can lead to system performance degradation[10–12].

This paper proposes a multi-stage optimization (MSO) method for map building of a multi-robot system. Considering a real environment, the process of building a global map for the multi-robot system is divided into the single-robot map acquisition stage, the multi-robot map transmission stage, and the multi-robot map merging stage.

To improve the efficiency of map transmission, we first selected a local map within a certain range of the robot according to the location. Considering that the robot is in an unknown environment, the uncertainty of its positioning will increase the difficulty of map building, which may eventually lead to a useless and inaccurate global map. The proposed method adopts the extended Kalman filter (EKF) to enhance the accuracy of the single robot positioning estimation, thereby improving the accuracy of map building during the local map acquisition stage.

Second, considering the robustness of the multi-robot system in the real environment, the MSO method takes the dynamic self-organized communication topology (DSCT), which adaptively adjusts the communication topology in response to changes in the network to improve the effectiveness and accuracy of the multi-robot map transmission stage.

Finally, considering the characteristics of the indoor environment, a multi-layer information filter (MLIF) is designed to filter the incorrect information generated in the global map, thereby improving the accuracy of the multi-robot map merging stage.

A series of experiments are performed to verify the effectiveness of the proposed method. The experimental accuracy and efficiency results of the global map are compared with those of previous classic methods. In addition, the applicability of the method is also verified in a real environment. The experimental results show that the MSO method enables the multi-robot system to build a global map quicker and more accurately.

The remainder of this paper is organized as follows. Section 2 discusses the recent literature on map building. Section 3 introduces the key content of the method proposed in the paper in detail. Section 4 shows the experimental results and corresponding analysis. Finally, Section 5 presents the conclusion of this paper.

2 Related Work

The indoor environment is a structured environment with boundaries. A boundary refers to an obstacle in the target area that could not be crossed by multiple robots. A structured environment means that the environment can be divided into multiple rectangular sub-regions. As a typical environment, the indoor environment has captured a lot of attention in the problem of multi-robot map building[13–15]. Thus, map building in the indoor environment is a matter of concern.

Most map building methods are based on the occupancy grid map after simultaneous localization and mapping (SLAM) construction[16]. SLAM refers to the process of sensing the environment and fusing available sensor information to generate a consistent map[17]. With the emergence of cluster robots that require interaction, extensive research is being conducted to extend the SLAM problem to multiple robots called multi-robot SLAM (MRSLAM)[18]. In previous research, the method based on MRSLAM collaboration can be divided into sharing raw sensor data[19] or sharing processed maps[16]. Since the sharing of occupancy grid map has the advantages of saving bandwidth and reducing the processing of raw data, it has been extensively studied[17]. This method of sharing the occupancy grid map after MRSLAM processing is called map merging. Moreover, the multi-robot map merging has now attracted the attention of many researchers. It is applied to many environments, with the indoor environment being one of the classics.

The map merging problem is divided into two: merging with known initial positions and merging without known initial positions. The former can obtain the relative position of the robot before the exploration map task begins, while the latter requires calculating the relative position of the robot as the robot completes the task.

2.1 Merging with known initial positions

In the multi-robot system, the local map of each robot should be merged into a global map as soon as possible to obtain a consistent map to better coordinate the exploration of each robot. Knowing the relative position of each robot from the beginning can obtain the global map earlier. In such a way, the robots can be well-coordinated at the beginning[20–22]. The boundary refers to the part where the free area and the unknown area are connected[1]. Simmons introduced an optimization method, in which the local robot first builds a local map, reduces errors by matching laser scanning, and further improves the global map by the global map processing module[22]. Burgard proposed a method that discusses how to coordinate multiple robots to effectively explore the environment considering the cost of reaching the target point and its utility[21].

2.2 Merging without known initial positions

The premise of Section 2.1 requires a known initial position of the robots. Some papers discuss a more general situation of not knowing the relative initial position of the robot. This situation is generally divided into two categories: direct map merging and indirect map merging[23].

2.2.1 Direct map merging

Direct map merging refers to relying on sensors to calculate the map transformation matrix among robots, thus fusing to obtain a global map. The main situation includes map merging after the relative position estimation is obtained under the premise that the robots meet[24]. The method proposed by Howard et al.[25] has provided an effective online map merging algorithm, which obtains the relative position of robots when they meet to perform map merging and stitching. This situation limits the conditions for map merging, where the robot meets another robot at least once. In addition, it may cause a relatively low map merging efficiency for taking a long time before the meeting. Furthermore, some papers considered that in a map building process by one robot, the position of another robot is estimated to obtain the relative position between every two robots[26]. In addition, there are other methods for estimating the relative position among robots in recent years. For example, the robot can utilize visual sensors to observe each other and non-unique landmarks to determine the relative position of the robot. The maps are then merged by propagating the uncertainty[27].

2.2.2 Indirect map merging

Indirect map merging refers to estimating the relative position between local maps through the characteristics of the overlapping parts between the local maps, and then performing map merging to obtain the global map. The method proposed in Ref. [28] is based on the combination of the scale-invariant feature transform (SIFT) and the iterative closest point algorithm to achieve the merge of local maps. A multi-robot map merging method based on speeded up robust features (SURF)[29] determines a master robot coordinate system and then performs rigid body transformation on the remaining slave robot coordinate systems to convert the map merging problem into an image matching quasi-minimization problem. Another method also converts the map merging problem into an image registration problem, which finds the best solution by rotating and translating the local map[13]. A method was proposed to match the occupancy grid graph by finding the correspondence between sparse feature sets[30]. This method adopted the improved random sample consensus (RANSAC) algorithm to search for the dynamic number of the internally consistent subsets of feature pairs and then calculating the translation and rotation between the maps. However, this has been tested on a series of atlases without considering the multi-carrier control problem. In addition to the above merging methods for grid maps, there are also studies of map merging for geometric features. Some approaches fit the measured line segments in the building of the local map, which finds the geometric similarity of the local map according to the matching of points and lines[31,32]. Nevertheless, the geometric feature-based map merging method is not suitable for unstructured environments. Besides, whether it is a map merge algorithm based on grid maps or a map merge algorithm based on geometric features, most of the overlapping parts are required between local maps, and the accuracy of merging depends on the size of the overlapping parts. Thereby, the efficiency of map merging and the time of map merging will be most affected.

Table 1 lists the strengths and weaknesses of different

Table 1 Features of the algorithms used for map building in an unknown environment.

Algorithm		Feature
Knowing initial position		**Strengths:** The relative position of the local map can be obtained from the beginning to merge the global map. **Weaknesses:** There is a limitation on the need to know the relative position.
Unknowing initial position	Direct map merging	**Strengths:** There is no need to know the initial relative position between the robots. **Weaknesses:** It requires robots to meet at least once.
	Indirect map merging	**Strengths:** There is no need to know the initial relative position between the robots. **Weaknesses:** It is necessary to obtain the overlapping area between the local maps.

multi-robot map-building algorithms. In summary, the advantage of the method with a known initial position is that the relative position of the local map can be obtained from the beginning to merge the global map. This facilitates better coordination among multiple robots and promotes the effective completion of the task of building a map. However, the premise of map-building method with a known initial position is to know the relative positions of the robots at the beginning, which means a limitation. When the initial position is unknown, there is no way to obtain the relative position among robots. Most direct map merging methods require robots to meet at least once, which may take a long time, leading to inefficient map building. The indirect map merging method does not require robots to satisfy the condition of meeting at least once. However, it is necessary to obtain the overlapping area between the local maps so that the feature can be extracted based on the overlapping area. In addition, when the initial position is unknown, a global map could not be obtained from the beginning, and multiple robots could not be better coordinated. Thus, the efficiency of the map merging process is ignored. For an indoor environment, the coordination among multiple robots will greatly affect the mapping efficiency.

The indoor environment has many rectangular areas. The lack of communication between the exploration robots will lead the robot to repeatedly explore certain rectangular areas, thereby increasing the time to complete the map and reducing efficiency. Consequently, it requires each robot to share the local map in time to ensure effective communication. Moreover, the accuracy of the global map depends on the accuracy of SLAM construction. Thereby, the processing of the map after SLAM construction to ensure the accuracy of the map is also a problem that requires attention.

The communication limitation of the multi-robot system in the actual environment is also worthy of attention. The limited communication of the multiple robots in the swarm robotic exploration problem was discussed in Ref. [33]. This problem was expressed as an optimization problem and solved by an improved brain storm optimization (BSO) algorithm. BSO algorithm[34] is a common evolutionary algorithm in the field of optimization. Reference [35] considered the problem of attenuation of the communication signal through the wall, proposed an outdoor-indoor signal fading model, and made a decision-making scheme.

Considering the accuracy and effectiveness of map building and the communication problems in the actual environment, the MSO method in the indoor environment is proposed. This method considers the uncertainty of the real environment and optimizes the mapping process according to the number and order of robot participation to ultimately improve the accuracy of the global map.

3 Multi-Stage Optimization (MSO) Method

3.1 Framework of the MSO method

In the MSO method (Fig. 1), the map building process is divided into three different stages based on the relationship between the single robot and the multiple robots in the multi-robot system: (1) the extended Kalman filter (EKF) in the single-robot map acquisition stage, (2) the DSCT in the multi-robot map transmission stage, and (3) the MLIF in the multi-robot map merging stage. In the multi-robot system, each stage cooperates to complete the task of building a global map in the indoor environment.

For the single-robot map acquisition stage, we

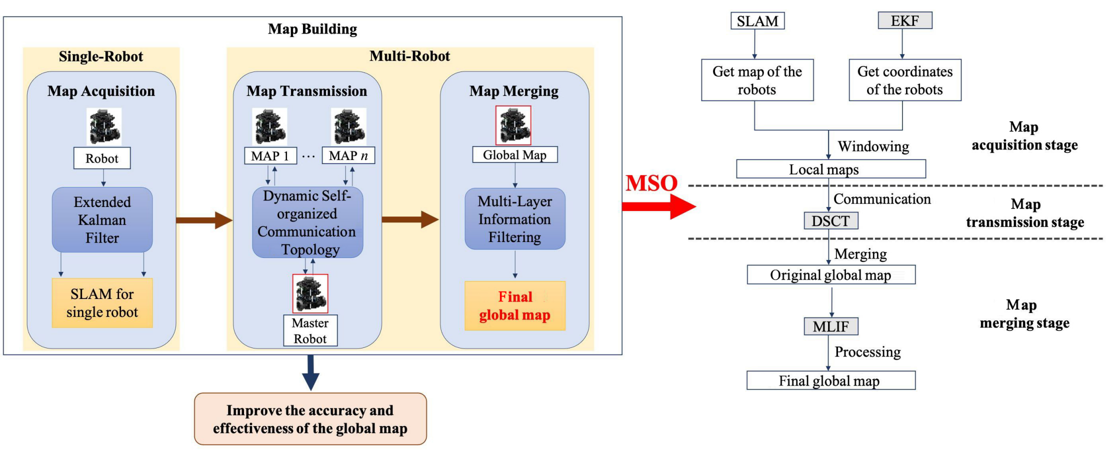

Fig. 1 Framework of the MSO method.

first optimize the global map from the single robot perspective. According to the process of obtaining the local map, the accuracy of the global map is based on the positioning result of the robots. When the robots travel through an unknown environment, the uncertainty over their positioning increases and the building of a global map becomes arduous. To improve the accuracy of a local map by the single robot, the MSO method uses the EKF. The EKF integrates the wheel odometry information and laser odometry information of the robot to output more accurate positioning results, thereby improving the accuracy of map building for the single robot. Second, in the multi-robot map transmission stage, the MSO method uses the DSCT to add a dynamic self-organized mechanism based on a basic communication network to deal with the failure of the robots. To allow robust communication between the robots, the MSO method predicts the dynamic changes in the building process of a global map and sets a backup master to complete the transfer of the topology center. Finally, the MSO method uses the MLIF to optimize the global map in the multi-robot map merging stage. The MLIF depicts and optimizes different erroneous information through different layers, filters the map in order, and then outputs a global map with higher precision.

3.2 EKF in the map acquisition stage

Because the unknown grid occupies most of the map generated by SLAM and the occupancy grid map retains the previously updated grid information every time, direct transmission and merging of the map built by SLAM will have a lot of invalid information. Considering that SLAM builds maps based on radar laser, the information within a certain range around the robot is valid. Dividing the local area and transmitting them after can ensure that the map information is updated while using a certain amount of communication data. Therefore, in the map acquisition stage, this work first uses the radar laser of the robot to build an occupancy grid map and then obtain the current position of the robot through EKF. A window is added to the occupancy grid map based on the map and location of the robot to obtain the local map around each robot and then carry out subsequent transmission.

Through the EKF, the robot can obtain more accurate positioning information under a limited sensor accuracy. The EKF is divided into two parts: prediction and measurement, which are defined by Eqs. (1) and (2), respectively. Here, Eq. (1) is approximated as a linear equation with an independent variable x_{t-1}, and Eq. (2) is approximated as a linear equation with an independent variable x_t.

$$g(u_t, x_{t-1}) = g(u_t, \mu_{t-1}) + W_t(x_{t-1} - \mu_{t-1}) \quad (1)$$

$$z_t = h(\bar{\mu}_t) + H_t(x_t - \mu_t) \quad (2)$$

where g is the prediction function, h is the measurement function, W_t is the state transition, and H_t is the observation matrix.

Equations (3)–(7) present the specific updating process of the EKF. Equations (3) and (4) show that the state at the current moment can be predicted by the state $(\mu_{t-1}, \Sigma_{t-1})$ at the previous moment $t-1$ and the control quantity u_t at the current moment t. μ_{t-1} refers to the mean of the stake and Σ_{t-1} refers to the covariance of the state. The predicted state refers to the Gaussian function determined by $\bar{\mu}_t$ and $\bar{\Sigma}_t$, as shown in Eqs. (3) and (4). The former represents the estimated value, while the latter represents the uncertainty. The Kalman filter gain K_t is updated as in Eq. (5). Equations (6) and (7) are the state outputs after the comprehensive prediction and measurement, i.e., the filtered output of the EKF.

$$\bar{\mu}_t = g(u_t, \mu_{t-1}) \quad (3)$$

$$\bar{\Sigma}_t = W_t \Sigma_{t-1} W_t^{\mathrm{T}} + R_t \quad (4)$$

$$K_t = \bar{\Sigma}_t H_t^{\mathrm{T}} (H_t \bar{\Sigma}_t H_t^{\mathrm{T}} + Q_t)^{-1} \quad (5)$$

$$\mu_t = \bar{\mu}_t + K_t(z_t - h(\bar{\mu}_t)) \quad (6)$$

$$\Sigma_t = (I - K_t H_t)\bar{\Sigma}_t \quad (7)$$

where R_t is the uncertainty of prediction and Q_t is the uncertainty of measurement at moment t.

Figure 2 shows the specific flowchart of this process. As shown in Fig. 2, the wheel odometry estimates the relative position of the robot according to the number of turns of the wheel. The laser odometry processes the scanned laser data, matches the position transformation of consecutive frames, and obtains the relative position transformation by an incremental method. The advantage of the wheel odometer is that

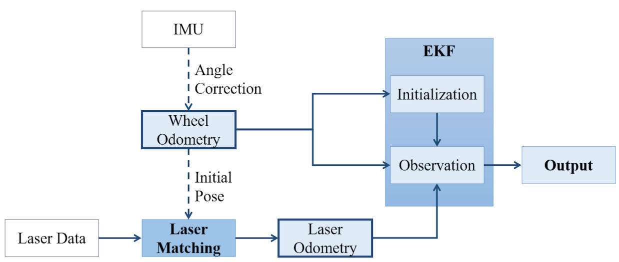

Fig. 2 Flowchart of the EKF process.

the sampling frequency is high, and the relative position of the robot can be measured in a short time. However, in reality, the wheels always spin and slip, resulting in significant deficiencies in the positioning accuracy. Fortunately, the laser odometer is not affected by the wheel condition. The EKF can compensate for the error of the situation, thereby improving the positioning accuracy and ultimately improving the accuracy of the local map.

3.3 DSCT in the map transmission stage

For the multi-robot system to complete the map building in the real environment, communication robustness is a key point that needs to be paid attention to. We first construct a basic communication network, and then design a dynamic communication network that has a self-organized topology to deal with the complexity and variability of the real environment (Fig. 3).

The basic communication network refers to the collaborative mechanism of robots under stable communication conditions. As shown in Fig. 3, the MSO method builds a centralized system based on the master and slave sketch. The master robot has the advantages of simple implementation and ensuring the optimality of the entire task. The exploration robot $r_1, \ldots, r_i$ obtains the local map through the first stage and then transmits it to the master robot r_0. The master robot r_0 sends the global map to each exploration robot in time to facilitate its further path planning. This collaborative framework guarantees the effective execution of global map building in the multi-robot system.

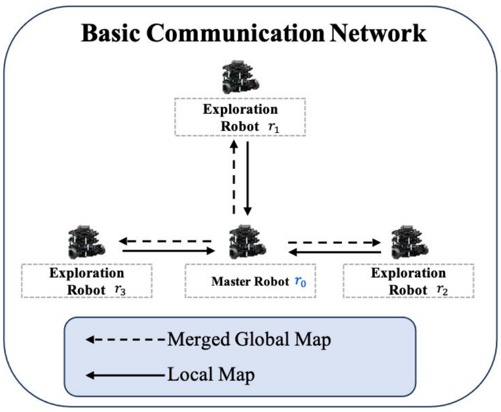

Fig. 3 Basic communication network.

However, the communication network could not always remain stable in a real environment. Therefore, it is necessary to consider possible changes in the network caused by insufficient battery power of the robot, sudden network failure, etc. Table 2 summarizes the possible emergencies. The MSO method adopts the DSCT for handling these uncertainties. The process in Fig. 4 shows the specific content of DSCT.

Figure 4 shows the decision-making process of the DSCT in the MSO method. The DSCT maintains a robot list in the communication network on the master

Table 2 Possible emergencies and their specific situations are reflected in the network.

Possible emergency	Reflected robot network situation
• New robot requests to join the network • Unstable communication environment	(1) Exploration robot enters the network
• Program failure of robots • Robot shuts down without power • Unstable communication environment	(2) Exploration robot exits the network
• Program failure of robots • Robot shuts down without power • Unstable communication environment	(3) Master robot exits the network

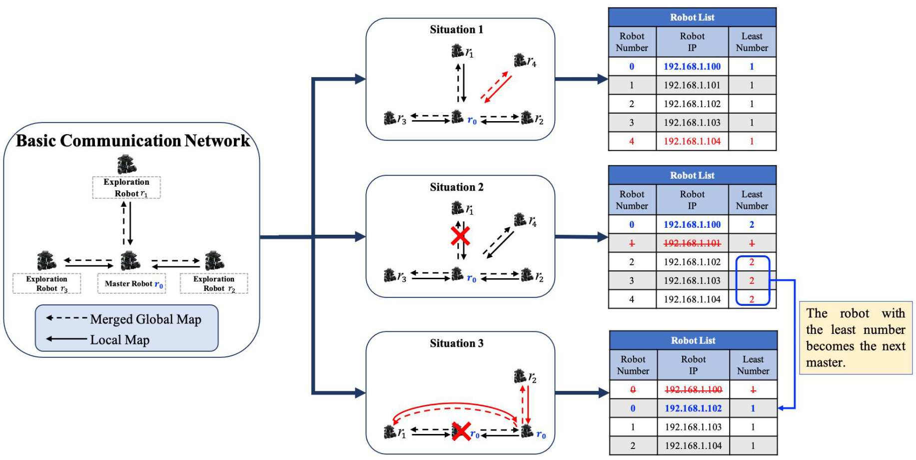

Fig. 4 Process of the DSCT in the MSO method. In the robot list, the blue value represents the master robot in the network, the black value represents the unchanged part, and the red value represents the current changed part.

robot r_0, and records the robot number, the robot IP, and the least number of all exploration robots during the process of organizing the network. The changes in the multi-robot communication network mainly include three situations: (1) the exploration robot enters the network, (2) the exploration robot exits the network, and (3) the master robot exits the network.

In a situation where the exploration robot enters the network, a connection between the master robot and the new exploration robot is created in the network on the premise that the previous master and slave sketch remains unchanged. For example, the master robot r_0 receives a request for joining the network from r_4, adds the number and IP of r_4 to the robot list, and the least number in the network remains unchanged. The remaining exploration robots will not be affected and continue completing their tasks.

For the situation where the exploration robot exits in the network, the master robot updates the network structure, deletes the connection with the exploration robots that have exited the network, and informs other exploration robots. For example, after the master robot r_0 has not received the information from r_1 for a long time, it will assume that r_1 is malfunctioning, cuts off the connection with it, and informs other exploration robots. The master robot r_0 deletes the information of r_1 in the robot list and checks whether the least number in the network needs to be updated.

When the master robot withdraws from the network, the previous master and slave sketch are destroyed, and the exploration robots determined by the least number need to rebuild a new star topology network. For example, when all exploration robots have not received information from the master robot r_0 for a long time, it will assume that r_0 loses connection. r_2, which is determined by the least number, will automatically become the next master robot and assume the task of re-networking. The new master robot will inherit the global map merged by the previous network and continues to complete map building and environmental exploration tasks.

Through the DSCT in the MSO method, the collaboration of robots will not be affected by the communication quality of the real environment, and the task of building a global map can be completed. This method guarantees the effectiveness of multi-robot map building.

3.4 MLIF in the map merging stage

In the multi-robot map merging stage, the proposed method adopts the MLIF to improve the accuracy of the global map. The global map built by the multi-robot system will produce incorrect information, such as non-connected domain information, dynamic obstacle information, and static non-smooth obstacle information. Considering the rules generated by the actual situation of multi-robot exploration in the indoor environment, we filter the global map to eliminate the incorrect grid state. Figure 5 shows the specific process.

The set of exploration robots in the multi-robot system is $R = \{r_i\}^n$, where n is the number of exploration robots, and $n \geqslant 2$. The local map and grids updated by r_i are respectively represented by M_t^i and G_t^i, and $G\_P_t^i$ is the set of path grid points for r_i in the t-th step. According to the characteristics of multi-robot exploration, the specific rules for map building could be summarized as follows:

Rule 1: The grid status after the obstacle cannot be updated, i.e., the grid updated must be in the same connected domain as the exploration robot.

$$G_t^i \subseteq M_t^{i\_c} \tag{8}$$

Here, $M_t^{i\_c}$ is the set of free grids points in the same connected domain as r_i in M_t^i in the t-th step.

Rule 2: The grids covered by the path of the exploration robots are in the same connected domain as the exploration robots.

$$G\_P_t^i \subseteq M_t^{i\_c} \tag{9}$$

Rule 3: When the grid point results are inconsistent, the judgment results of most exploration robots can represent the final state of the grid.

$$G_t = \frac{1}{k}\sum_{i=1}^{k} G_t^i \tag{10}$$

Here, k represents the number of times that the grid G_t is updated before the t-th step.

Rule 4: The shape of the actual static obstacle is smooth.

According to the above rules, we use different approaches to solve different types of error information in the global map. In Rule 1, the connected domain judgment is used to filter out the incorrect feasible domain map information outside the obstacle. For non-connected domain information, we mark the connected domains of the free areas of the global map and record the connected domain number of the exploration robot location. The free grids with inconsistent numbers are

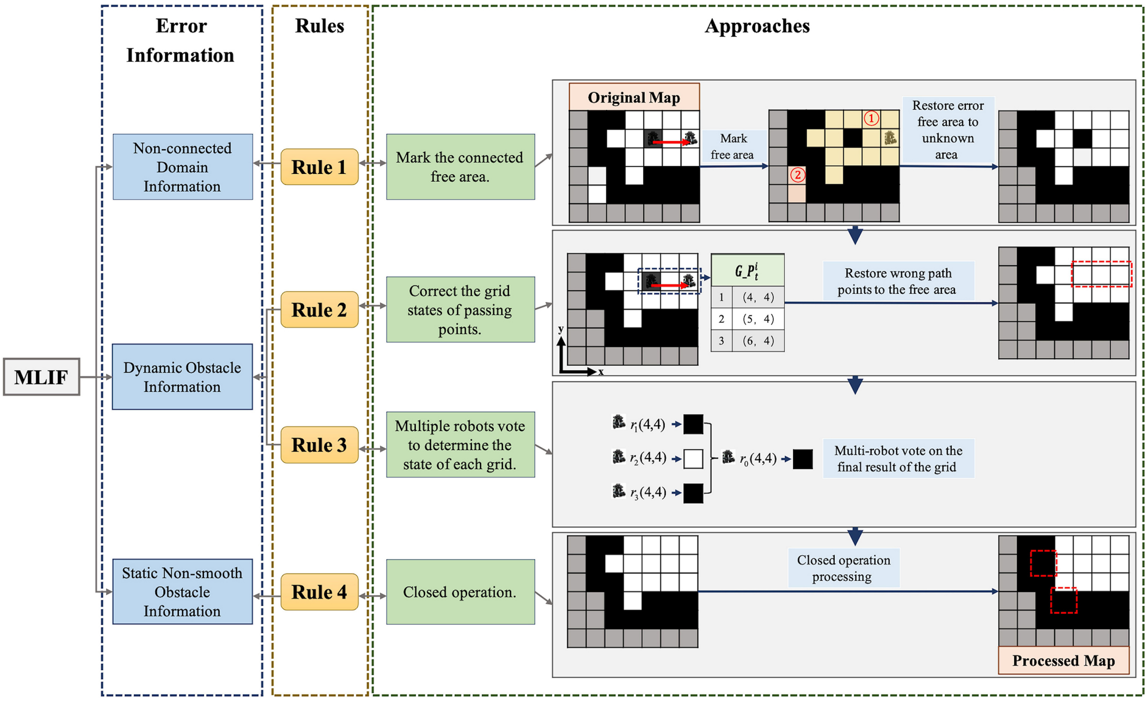

Fig. 5 MLIF framework in the MSO method. Error information refers to some errors that can be corrected in the process of building a global map. According to the four different rules, four filter layers with different approaches are added.

considered error grids, which are corrected to unknown grids.

In Rules 2 and 3, the dynamic obstacle information includes two situations. One is the occupied grids covered by the path of exploration robots. In this case, we record the path point of each exploration robot and remove the occupied grids in the fixed area around each sampling point. The second situation is that different exploration robots have different judgment results for the same grid. For this situation, we trust the sensor measurement results of most exploration robots. Therefore, we use multi-robot voting to take the average value to determine the value of each grid.

In Rule 4, static obstacles with uneven edges should be processed. For the static non-smooth obstacle information, we first provide a closed operation to expand the global map and then perform the corrosion operation to smooth the edges of the static obstacle.

According to the four rules, the MSO method can correct the incorrect information according to the rules of the real environment through the MLIF, thereby obtaining a more accurate global map.

To summarize, the MSO method uses the EKF in the map acquisition stage, the DSCT in the map transmission stage, and the MLIF in the map merging stage to improve the accuracy, efficiency, and effectiveness in building a global map.

4 Experiment and Analysis

We carry out the experimental results both in the Gazebo platform and real indoor environment to show the performance of the proposed method. For the Gazebo platform, we design different types and sizes of complex indoor environments to illustrate the feasibility and effectiveness of the proposed method in the indoor environment. We focus on the accuracy and exploratory efficiency of the MSO method with other algorithms, such as the known initial position method (KIPM) and the unknown initial position method (UIPM) in the paper[8]. These algorithms use the same boundary exploration method[36], in which each exploration robot searches for the nearest boundary and explores based on the map it acquires. Considering the size of the robot and the grid, when the continuous grid of the boundary is less than or equal to a certain number, it will not be recorded as the boundary.

For actual scenarios, to illustrate the applicability of the method in the real environment, we verify the positioning accuracy, test the stability of the communication network, and show the mapping results in a real environment.

The type of robot selected in the experiment is Turtlebot3 Burger (Fig. 6), and the size of the robot is 138 mm ×178 mm × 192 mm.

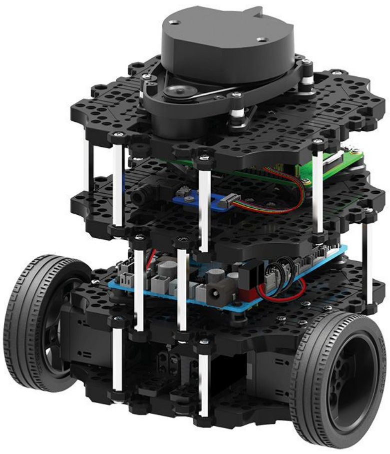

Fig. 6 Turtlebot3 Burger robot.

4.1 Performance index

The performance indicators to evaluate the accuracy and effectiveness of the global map are designed. The specific evaluation content and indicators are as follows.

4.1.1 Accuracy of the global map

In the Gazebo platform, we took a two-dimensional grid map of the environment as the comparison object. We evaluated the structural similarity (StS) between the global map built by different algorithms and the two-dimensional grid map of the environment. Therefore, the StS of the global maps is defined as Eq. (11).

$$\mathrm{StS} = \frac{\sum_m \sum_n (A_{mn} - \bar{A})(B_{mn} - \bar{B})}{\sqrt{(\sum_m \sum_n (A_{mn} - \bar{A})^2)(\sum_m \sum_n (B_{mn} - \bar{B})^2)}} \tag{11}$$

where $A_{m,n}$ and $B_{m,n}$ represent the two-dimensional matrix of the single-robot occupancy grid map and multi-robot occupancy grid map, respectively. StS represents the accuracy of the global map. A and B represent the two-dimensional matrix of the single-robot occupancy grid map and multi-robot occupancy grid map, respectively. $\bar{A}$ represents the mean of array A and $\bar{B}$ represents the mean of array B.

In addition, the free area is very important, which affects the judgment of the exploration robots. Therefore, we also evaluated the accuracy of the map building from the false positive rate (FPR) of the free area.

$$\mathrm{FPR} = \frac{num_{F\_N}}{num_{F\_S} + num_{F\_N}} \tag{12}$$

where F_S represents the free grids in the same connected domain with exploration robots, and F_N represents the free grids that are not in the same connected domain with the exploration robots. num_{F_N} is the number of F_N, and num_{F_S} is the number of F_S.

4.1.2 Efficiency of the global map

We choose the time to explore the global map (TEGM), and the average exploration rate (AER) to quantitatively describe the efficiency of the mapping process. The AER can be calculated by the average of the number of exploration grids num_{ne} at the later moment minus the number of exploration grids num_{pr} at the previous moment. Equation (13) shows the calculation of AER.

$$\mathrm{AER} = \frac{\sum_1^N (num_{ne} - num_{pr})}{t} \tag{13}$$

where N represents the final exploration time, and t represents the duration of exploration.

4.2 Experimental results in the Gazebo platform

Since the sensors of the exploration robots and communication environment are in stable conditions in the Gazebo platform, it is not necessary to test the EKF and the DSCT. In this section, we mainly tested the performance of the MLIF in the MSO method from the perspective of accuracy and efficiency.

4.2.1 Comparison for accuracy of the global map

The experimental results are presented from two aspects: the StS and the FPR. We constructed ten different environments and compared the accuracy of the three algorithms. In ten environments, the initial positions (IniP) of three exploration robots are the same. In addition to comparing different environments in the vertical direction, the same environment was also compared in the horizontal direction. We chose a different IniP in the same environment to compare the accuracy of the map.

First, for the StS, three exploration robots in 10 different environments are compared and the results are shown in Table 3. For the sake of fairness, the global maps were all clipped so that the indoor environment is located at the same location throughout the map. The covariance of the map built by the three algorithms and the map built by the single robot is used to represent the StS. The range of StS is between $[-1, 1]$, the closer the StS value to 1, the greater the similarity between the two graph structures.

The higher the StS value, the more similar is the mapping result to the real map. The highlighted results in Table 3 show the best experimental results in each experiment. It is evident that among ten experiments, the StS of the MSO method is the largest in nine experiments, which proves that the map built by the MSO method is more similar to the true value of the environment.

More than the longitudinal experiments, horizontal

Table 3 Comparison of StS in different environments.

Environment	MSO	KIPM	UIPM
1	**0.4873**	0.4358	0.4776
2	**0.4110**	0.2653	0.3335
3	**0.4982**	0.3092	0.0970
4	**0.5279**	0.3574	0.4054
5	**0.3098**	0.3066	0.1839
6	**0.5096**	0.1806	0.1581
7	**0.4362**	0.2613	0.4217
8	**0.3547**	0.3135	0.3159
9	0.2804	**0.3231**	0.2551
10	**0.2107**	0.1959	0.1977

experiment comparisons are also conducted. We performed 14 experiments by varying the IniP value in the same environment. Table 4 shows the results.

The highlighted results in Table 4 represent the best results in different environments. All experimental results show that for different IniP values in the same environment, the MSO method has a relatively high StS, which means that the map built by the MSO method has higher accuracy. As can be seen from Tables 3 and 4, whether it is in different environments or there are different IniP values in the same environment, the MSO can obtain relatively high accuracy in most cases.

Furthermore, Table 5 lists the comparison results of each algorithm in the FPR. These are the results of the three exploration robots building maps in the previous ten environments. The MSO method performs the MLIF on a global map, which effectively reduces the FPR of the free area.

The smaller the FPR, the higher the accuracy of the

Table 4 Comparison of StS in the same environment.

IniP	MSO	KIPM	UIPM
IniP1	**0.3191**	0.3071	0.2886
IniP2	**0.2818**	0.2731	0.1787
IniP3	**0.4626**	0.3748	0.2609
IniP4	**0.3987**	0.3893	0.3782
IniP5	**0.4421**	0.3334	0.2767
IniP6	**0.3935**	0.3188	0.2790
IniP7	**0.4107**	0.3512	0.1448
IniP8	**0.3183**	0.3137	0.0698
IniP9	**0.2344**	0.1407	0.1008
IniP10	**0.2817**	0.2201	0.1426
IniP11	**0.4059**	0.2458	0.3368
IniP12	**0.3057**	0.3014	0.1103
IniP13	**0.4316**	0.2525	0.3622
IniP14	**0.4399**	0.3697	0.4362
AVERAGE	**0.3661**	0.2994	0.2404
MAX	**0.4626**	0.3893	0.4362
MIN	**0.2344**	0.1407	0.0698

Table 5 Comparison of FPR of the free area. (%)

Environment	MSO	KIPM	UIPM
1	**0.00**	5.10	0.81
2	**0.00**	4.89	8.27
3	**0.00**	2.63	2.03
4	**0.00**	1.57	0.37
5	**0.00**	1.73	0.86
6	**0.00**	15.12	1.89
7	**0.00**	2.09	0.78
8	**0.00**	2.41	3.17
9	**0.00**	2.30	1.12
10	**0.00**	2.21	3.97

map building. Table 5 highlights the best results in each experiment. The FPR in MSO can be minimized because MLIF is used to filter the error information in the global map. Therefore, the MSO method can improve the accuracy of the final global map.

4.2.2 Efficiency comparison of a global map

To verify the efficiency of the MSO method, we compared the efficiencies of the map building between different algorithms. In this part, we compared the KIPM without the cooperation and the MSO with a communication network in four indoor environments (Fig. 7). The IniP of three exploration robots is changed eight times in each environment. The experimental results are presented from two aspects: the TEGM and the AER.

First, we set a time node every 5 seconds and recorded the time node when the environment is completely explored in each experiment. Figure 8 shows the results of the above 32 groups of the experiments.

Figure 8 shows that when considering the TEGM, the MSO is superior to the KIPM in 32 situations. In the best

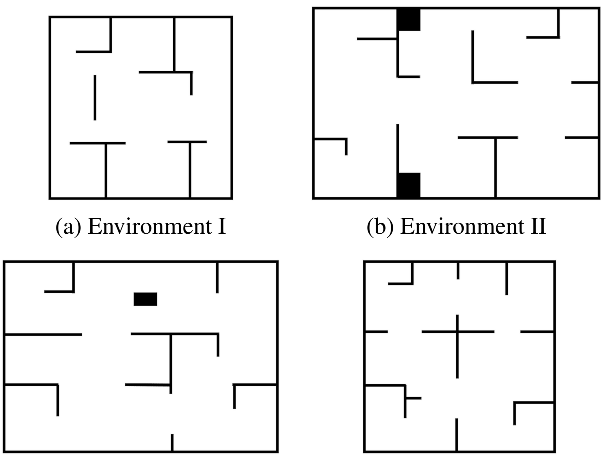

(a) Environment I (b) Environment II (c) Environment III (d) Environment IV

Fig. 7 Simulation environments.

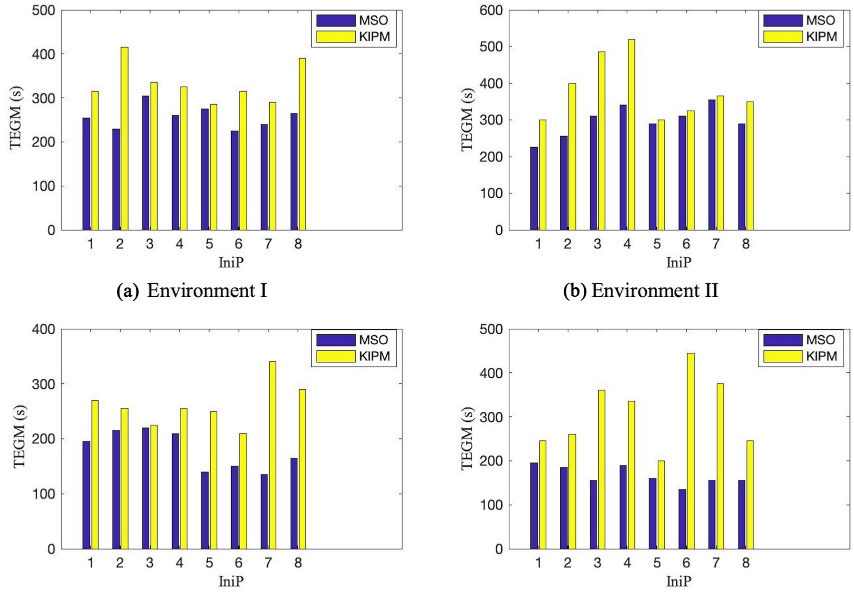

(a) Environment I (b) Environment II

(c) Environment III (d) Environment IV

Fig. 8 Comparison of TEGM in four environments.

case, the MSO is 5 seconds faster than the KIPM, which is within an acceptable range. Nevertheless, in the worst case, the MSO is 310 seconds faster than the KIPM. Obviously, the TEGM will be unstable and inefficient without a communication network.

Table 6 shows the AER. A higher AER means that the algorithm has a higher mapping efficiency. In 32 experiments, the AER of the MSO is all better than the KIPM, which proves that the MSO has higher efficiency. Through the AER of the multi-robot system, a consistent conclusion can be obtained.

4.2.3 Performance validation for more robots

To verify the generalization ability of the method in the multi-robot system, we changed the number of exploration robots and verified whether the algorithm is still applicable in more exploration robot systems. Five exploration robots conducted experiments on the four environments mentioned in Section 4.3, and we changed eight different IniP values in each environment. In this section, we chose the StS as the accuracy performance index and the TEGM as the efficiency performance index.

For global map accuracy, we compared the StS values of five exploration robots, and the results are shown in Table 7.

As observed from Table 7, the MSO performed best among the three algorithms in 21 experiments out of 24 experiments. This means that it has a higher similarity with the true value of the environment, thus proving that the mapping results of the MSO have higher accuracy.

For global map efficiency, Fig. 9 shows the comparison of the TEGM in four environments. The graph shows that in the system of five exploration robots, the MSO can quickly complete the task of exploring the global environment. To prove the effectiveness of the MSO more comprehensively, we also compared the TEGM of different numbers of exploration robots in

Table 6 Comparison of AER.

(grid/s)

IniP	Environment I		Environment II		Environment III		Environment IV	
	MSO	KIPM	MSO	KIPM	MSO	KIPM	MSO	KIPM
IniP1	**114.93**	78.371	**157.186**	148.750	**108.137**	98.224	**101.054**	95.989
IniP2	**122.522**	112.739	**138.055**	127.851	**96.838**	90.086	**113.168**	109.400
IniP3	**88.797**	82.737	**113.303**	102.190	**98.874**	91.056	**130.820**	113.548
IniP4	**114.267**	108.416	**108.397**	89.523	**117.453**	115.430	**107.222**	97.643
IniP5	**108.815**	101.127	**124.008**	105.954	**136.836**	131.297	**116.350**	108.600
IniP6	**119.747**	94.058	**115.384**	109.148	**126.945**	122.662	**153.840**	118.800
IniP7	**121.091**	114.038	**101.794**	98.551	**161.346**	150.777	**141.269**	135.972
IniP8	**103.480**	95.713	**125.250**	120.604	**127.500**	120.360	**119.867**	114.740

Table 7 Comparison of StS in different environments (five exploration robots).

Environment		MSO	KIPM	UIPM
I	IniP1	**0.4342**	0.1012	0.2367
	IniP2	**0.4677**	0.4344	0.3048
	IniP3	**0.4357**	0.2427	0.3072
	IniP4	**0.3319**	0.2245	0.3234
	IniP5	0.3708	**0.4615**	0.2813
	IniP6	**0.1911**	0.1354	0.0881
II	IniP1	**0.4391**	0.0122	0.2650
	IniP2	**0.2876**	0.1325	0.2608
	IniP3	**0.4113**	0.3351	0.2873
	IniP4	**0.4507**	0.2505	0.0910
	IniP5	**0.3779**	0.3205	0.3722
	IniP6	**0.4236**	0.2091	0.1213
III	IniP1	0.3387	**0.4370**	0.2173
	IniP2	**0.1571**	0.1211	0.0842
	IniP3	**0.4851**	0.1658	0.1250
	IniP4	0.4203	**0.4664**	0.4349
	IniP5	**0.2008**	0.0850	0.1143
	IniP6	**0.4685**	0.1904	0.0919
IV	IniP1	**0.4326**	0.4283	0.0865
	IniP2	**0.4468**	0.3981	0.3120
	IniP3	**0.4540**	0.4339	0.4181
	IniP4	**0.5464**	0.3383	0.2386
	IniP5	**0.5271**	0.2245	0.5006
	IniP6	**0.5212**	0.2066	0.2497

the same environment. The TEGM for eight groups of exploration robots in four environments to build the global map is averaged. Table 8 shows the comparison results.

The TEGM of five exploration robots is not significantly shorter than that of the three exploration robots. Increasing the number of exploration robots does not present a shorter exploration time. The reason for this situation is related to the size of the map. Increasing the number of exploration robots when the map is limited will not shorten the exploration time. Because the possibility of exploration robots repeatedly exploring a certain path becomes higher, it does not reflect the advantages of increasing the exploration robots.

To further illustrate the effectiveness of the algorithm in the multi-robot system, we set up a more complex environment to carry out experiments on different numbers of exploration robots. Figure 10 shows the larger environment.

We conducted a comparative analysis of the system of seven exploration robots in Environment V and compared them with the system of five exploration robots and three exploration robots. Figure 11 shows the comparison results.

In Environment V, no matter how many exploration robots are present, the MSO can build a global map faster

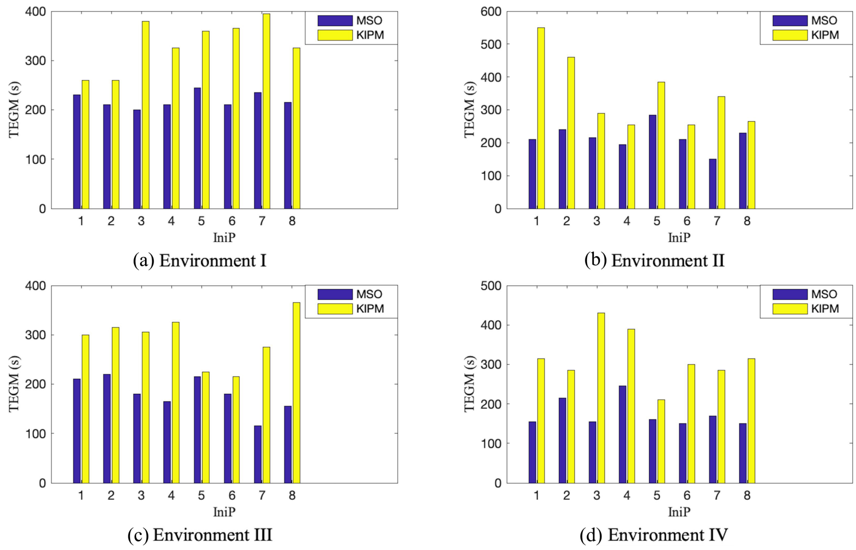

Fig. 9 Comparison of TEGM in four environments (five exploration robots).

Table 8 Average TEGM of different numbers of exploration robots in the same environment. (s)

Number of robots	Environment I		Environment II		Environment III		Environment IV	
	MSO	KIPM	MSO	KIPM	MSO	KIPM	MSO	KIPM
3	**256.875**	333.750	**296.875**	380.625	**178.750**	261.875	**166.250**	308.125
5	**219.375**	333.750	**263.125**	361.875	**180.000**	290.625	**175.000**	316.250

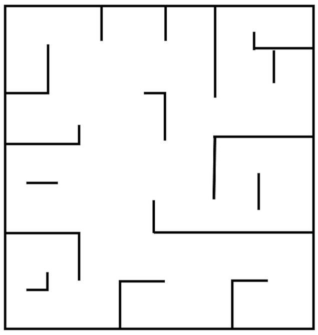

Fig. 10 Environment V.

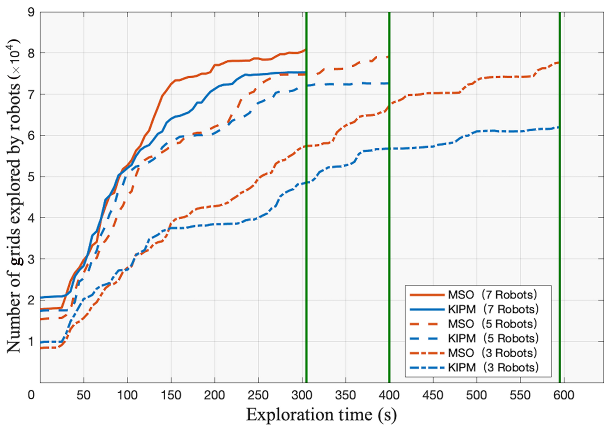

Fig. 11 Comparison of TEGM in Environment V (s).

than the KIPM. Moreover, the performance of seven exploration robots is better than that of five exploration robots and three exploration robots, indicating that with the increase of the environment size, the increase in the number of exploration robots will help the system to explore the environment faster.

4.3 Applicability of the method in actual scenarios

To examine the effectiveness of the proposed method in a real environment, we compared and analyzed the positioning accuracy and communication stability. For the positioning accuracy, we compared the EKF positioning results with the positioning results of the other three algorithms. The real position is marked, and the absolute position difference of each marked point is recorded and averaged. For the effectiveness of the communication, we tested the measures taken by the MSO method when the network fails during map building in a real environment.

Additionally, we displayed the MSO mapping process in the real environment to prove the effectiveness of the MLIF.

4.3.1 Analysis of the positioning error for a single exploration robot

We compared the EKF fusion results with the wheel odometer results and the two different separate laser odometers are denoted as VO and RFTO, respectively. We ran five experiments on the same map and recorded the absolute error of all marked points in each experiment, as shown in Fig. 12. We then counted the average error and total average error of each algorithm

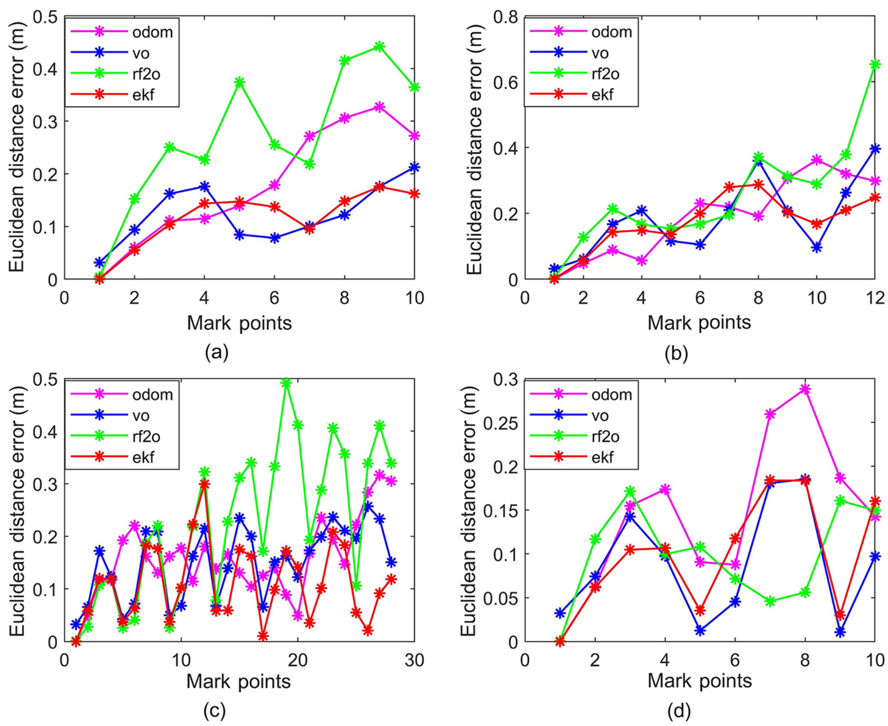

Fig. 12 Comparison of absolute errors of 4 experiments.

in each experiment, as shown in Table 9.

Figure 12 and Table 9 indicate that based on the results of the four tests and the final average value, the use of EKF can reduce the positioning error in the real environment. Although the EKF in Test 4 is not optimal, it is not much different from that of the optimal result. Improvement of the positioning accuracy will improve the accuracy of SLAM to build local maps, which can prove the necessity of the MSO method to use the EKF for information fusion.

4.3.2 Analysis of the impact for dynamic network

For communication stability, we separately tested the specific performance of the communication network in three emergencies: the exploration robot entering the network, the exploration robot exiting the network, and the master robot exiting the network. In the experiment, a process of network dynamic change is shown in Table 10.

According to Table 10, the multi-robot system will not be affected by unexpected robot accidents and can complete the task of building a global map. This confirmed the stability of the communication network in the MSO method.

4.3.3 The mapping process in the real environment

We tested the usability of the method in a 3 m $\times$ 3 m real environment. Figure 13 shows the process of building a global map. First, three robots start from three different initial positions. Then, the robots continue to supplement the global map as they explore. In this process, some errors will be generated. Finally, the MSO method uses MLIF to process the global map after the exploration task is completed. It can be seen that the MLIF in the MSO method can eliminate erroneous information in the mapping process, and the MSO can guide multi-exploration robots to build a global map in the real environment.

Table 9 Average error and total average error of each algorithm in each experiment.

Experiment	ODOM	VO	RF2O	EKF
1	0.1781	0.1237	0.2704	**0.1167**
2	0.1894	0.1851	0.2525	**0.1733**
3	0.1585	0.1508	0.2215	**0.1111**
4	0.1446	**0.0878**	0.0981	0.0984
Average	0.1677	0.1369	0.2106	**0.1249**

5 Conclusion

This paper proposes a map-building method for a multi-robot system named the MSO method. Through this method, the multi-robot system can improve the accuracy, efficiency, and effectiveness of building a global map. The method considers different stages of map building: the EKF in the map acquisition stage, the DSCT in the map transmission stage, and the MLIF in the map merging stage. The EKF in the map acquisition stage is used to fuse the position estimates given by different sensors to improve the accuracy of the exploration robot positioning, ensuring the accuracy of acquiring the map. In the second stage, the DSCT in the MSO method is established to ensure the effectiveness of map transmission and avoid the system paralysis caused by the robot failure in a real environment. Finally, the MLIF in the MSO is used in the map merging stage to process the error information generated in the previous two stages, improving the accuracy of the final global map.

Table 10 Process of network dynamic change.

Situation	Specific description	Robot list	Robot No.	Explanation
1	Exploration robot *1* enters the network.	1: {change number: 2, id: 1, number: 2}	1	New robot joins the network.
1	Exploration robot *2* enters the network.	1: {change number: 1, id: 1, number: 1} 2: {change number: 2, id: 2, number: 2}	1, 2	New robot joins the network.
1	Exploration robot *3* enters the network.	1: {change number: 3, id: 1, number: 3} 2: {change number: 3, id: 2, number: 3} 3: {change number: 3, id: 3, number: 3}	1, 2, 3	New robot joins the network.
2	Exploration robot *1* exits the network.	2: {change number: 1, id: 2, number: 2} 3: {change number: 1, id: 3, number: 2}	2, 3	Robot *1* exits the network.
1	Exploration robot *4* enters the network.	2: {change number: 4, id: 2, number: 3} 3: {change number: 4, id: 3, number: 3} 4: {change number: 4, id: 4, number: 3}	2, 3, 4	New robot joins the network.
3	Master robot *0* exits the network.	1: {change number: 2, id: 1, number: 2} 2: {change number: 2, id: 2, number: 2}	1, 2	Exploration robot *2* is the master, and the other robots are re-networked.

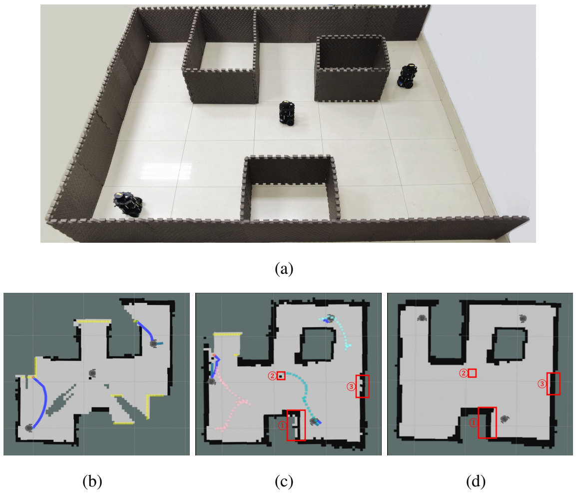

Fig. 13 Process of building a map by three robots in a real environment. (a) The real environment in which the multi-robot system experiments. Yellow points denote the edge points. (b) Exploration robots plan the route separately at IniP. (c) An intermediate stage of the multi-robot system for map building. The marked points are the three types of incorrect information generated during the mapping process described by the MLIF. (d) Global map built by the multi-robot system through the MSO method. The marked points correspond to the three incorrect information in Fig. 13b, which shows that the MSO method adopts the MLIF to deal with the errors in the global map.

The experimental results demonstrate that the MSO method could effectively and accurately complete the task of building a global map by multiple robots in the indoor environment. Based on the Gazebo platform, its accuracy is proved to be better than other map merging algorithms, and the establishment of a communication network can improve the efficiency of the map-building process. In addition, we proved that the proposed method could improve the ability of multiple robots to build a global map in a real environment because it takes into account the positioning error and the communication environment.

Our future work will focus on three aspects. First, a better communication mechanism will be used to improve the stability and reliability of the map transmission. Then, we will apply the MSO method to other environments to verify its applicability. Finally, it is also indispensable to optimize the exploration method to improve the multi-robot exploration system.

Acknowledgment

This work was supported in part by the National Natural Science Foundation of China (Nos. 61671041 and 61806119) and the Shaanxi Key Laboratory of Integrated and Intelligent Navigation (No. SKLIIN-20190201).

References

[1] C. Robin and S. Lacroix, Multi-robot target detection and tracking: Taxonomy and survey, *Auton. Robots*, vol. 40, no. 4, pp. 729–760, 2016.

[2] Y. Wang, G. Zheng, D. Efimov, and W. Perruquetti, Improved altitude control method with disturbance compensation for an indoor blimp robot, presented at 2017 IEEE 56th Annu. Conf. Decision and Control, Melbourne, Australia, 2017, pp. 3902–3907.

[3] H. M. Gao, X. B. Zhang, J. Wen, J. Yuan, and Y. C. Fang, Autonomous indoor exploration via polygon map construction and graph-based SLAM using directional endpoint features, *IEEE Trans. Automat. Sci. Eng.*, vol. 16, no. 4, pp. 1531–1542, 2019.

[4] C. Q. Wang, D. L. Zhu, T. Li, M. Q. H. Meng, and C. W. de Silva, Efficient autonomous robotic exploration with semantic road map in indoor environments, *IEEE Rob. Automat. Lett.*, vol. 4, no. 3, pp. 2989–2996, 2019.

[5] C. Q. Wang, D. L. Zhu, T. Li, M. Q. H. Meng, and C. De Silva, SRM: An efficient framework for autonomous robotic exploration in indoor environments, arXiv preprint arXiv: 1812.09852, 2018.

[6] Q. L. Feng, H. Cai, Y. B. Yang, J. H. Xu, M. R. Jiang, F. Li, X. T. Li, and C. C. Yan, An experimental and numerical study on a multi-robot source localization method independent of airflow information in dynamic indoor environments, *Sustain. Cities Soc.*, vol. 53, p. 101897, 2020.

[7] B. F. Chen, S. Y. Li, H. W. Zhao, and L. M. Liu, Map merging with suppositional box for multi-robot indoor mapping, *Electronics*, vol. 10, no. 7, p. 815, 2021.

[8] J. Hörner, Map-merging for multi-robot system, https://is.cuni.cz/webapps/zzp/detail/174125/, 2016.

[9] J. G. Mangelson, D. Dominic, R. M. Eustice, and R. Vasudevan, Pairwise consistent measurement set maximization for robust multi-robot map merging, presented at IEEE Int. Conf. Robotics and Automation, Brisbane, Australia, 2018, pp. 2916–2923.

[10] Y. J. Wang, Y. D. Song, and F. L. Lewis, Robust adaptive fault-tolerant control of multiagent systems with uncertain nonidentical dynamics and undetectable actuation failures, *IEEE Trans. Indust. Electron.*, vol. 62, no. 6, pp. 3978–3988, 2015.

[11] J. W. Zhu, G. H. Yang, W. A. Zhang, and L. Yu, Cooperative fault tolerant tracking control for multiagent systems: An intermediate estimator-based approach, *IEEE Trans. Cybernet.*, vol. 48, no. 10, pp. 2972–2980, 2018.

[12] H. F. Cappel, A hierarchical multi-robot mapping architecture subject to communication constraints, arXiv preprint arXiv: 2102.01641, 2021.

[13] A. A. Ravankar, A. Ravankar, Y. Kobayashi, and T. Emaru, Cooperative multi-robot map merging with task distribution, in *Proc. JSME annual Conf. Robotics and Mechatronics 2019*, 2019, pp. 2A1–B15.

[14] J. L. S. Rincon and S. Carpin, Time-constrained exploration using toposemantic spatial models: A reproducible approach to measurable robotics, *IEEE Robot. Automat. Mag.*, vol. 26, no. 3, pp. 78–87, 2019.

[15] A. Q. Li, R. Cipolleschi, M. Giusto, and F. Amigoni, A semantically-informed multirobot system for exploration of relevant areas in search and rescue settings, *Auton. Robots*, vol. 40, no. 4, pp. 581–597, 2016.

[16] A. Birk and S. Carpin, Merging occupancy grid maps from multiple robots, *Proc. IEEE*, vol. 94, no. 7, pp. 1384–1397, 2006.

[17] S. Saeedi, L. Paull, M. Trentini, M. Seto, and H. Li, Group mapping: A topological approach to map merging for multiple robots, *IEEE Robot. Automat. Mag.*, vol. 21, no. 2, pp. 60–72, 2014.

[18] J. Kshirsagar, S. Shue, and J. M. Conrad, A survey of implementation of multi-robot simultaneous localization and mapping, presented at SoutheastCon 2018, St. Petersburg, FL, USA, 2018, pp. 1–7.

[19] L. Carlone, M. K. Ng, J. J. Du, B. Bona, and M. Indri, Simultaneous localization and mapping using rao-blackwellized particle filters in multi robot systems, *J. Intell. Robot. Syst.*, vol. 63, no. 2, pp. 283–307, 2011.

[20] Y. L. Liu, X. P. Fan, and H. Zhang, A fast map merging algorithm in the field of multirobot SLAM, *Sci. World J.*, vol. 2013, p. 169635, 2013.

[21] W. Burgard, M. Moors, C. Stachniss, and F. E. Schneider, Coordinated multi-robot exploration, *IEEE Trans. Robot.*, vol. 21, no. 3, pp. 376–386, 2005.

[22] R. Simmons, D. Apfelbaum, W. Burgard, D. Fox, M. Moors, S. Thrun, and H. Younes, Coordination for multi-robot exploration and mapping, in *Proc. AAAI National Conf. Artificial Intelligence*, Austin, TX, USA, 2000, pp. 852–858.

[23] H. C. Lee, S. H. Lee, T. S. Lee, D. J. Kim, and B. H. Lee, A survey of map merging techniques for cooperative-SLAM, presented at 2012 9^{th} Int. Conf. Ubiquitous Robots and Ambient Intelligence, Daejeon, South Korea, 2012, pp. 285–287.

[24] X. S. Zhou and S. I. Roumeliotis, Multi-robot SLAM with unknown initial correspondence: The robot rendezvous case, presented at 2006 IEEE/RSJ Int. Conf. Intelligent Robots and Systems, Beijing, China, 2006, pp. 1785–1792.

[25] A. Howard, L. E. Parker, and G. S. Sukhatme, Experiments with a large heterogeneous mobile robot team: Exploration, mapping, deployment and detection, *Int. J. Robot. Res.*, vol. 25, nos. 5&6, pp. 431–447, 2006.

[26] J. W. Fenwick, P. M. Newman, and J. J. Leonard, Cooperative concurrent mapping and localization, in *Proc. 2002 IEEE Int. Conf. Robotics and Automation* (*Cat. No. 02CH37292*), Washington, DC, USA, 2002, pp. 1810–1817.

[27] N. E. Özkucur and H. L. Akın, Cooperative multi-robot map merging using fast-SLAM, in *Robot Soccer World Cup*, J. Baltes, M. G. Lagoudakis, T. Naruse, and S. S. Ghidary, eds. Berlin, Heidelberg: Springer, 2010, pp. 449–460.

[28] K. Wang, S. M. Jia, Y. C. Li, X. Z. Li, and B. Guo, Research on map merging for multi-robotic system based on RTM, presented at 2012 IEEE Int. Conf. Information and Automation, Shenyang, China, 2012, pp. 156–161.

[29] H. W. Tang, W. Sun, K. Yang, A. P. Lin, Y. F. Lv, and X. Cheng, Grid map merging approach of multi-robot based on SURF feature, (in Chinese), *J. Electron. Meas. Instrum.*, vol. 31, no. 6, pp. 859–868, 2017

[30] J. L. Blanco, J. G. Jiménez, and J. A. Fernández-Madrigal, A robust, multi-hypothesis approach to matching occupancy grid maps, *Robotica*, vol. 31, no. 5, pp. 687–701, 2013.

[31] R. Xiong, J. Chu, and J. Wu, Incremental mapping based on dot-line congruence for robot, *Control Theory Appl.*, vol. 24, no. 2, pp. 170–176, 2007.

[32] R. Lakaemper, L. J. Latecki, and D. Wolter, Incremental multi-robot mapping, presented at 2005 IEEE/RSJ Int. Conf. Intelligent Robots and Systems, Edmonton, Canada, 2005, pp. 3846–3851.

[33] G. Li, D. B. Zhang, and Y. H. Shi, An unknown environment exploration strategy for swarm robotics based on brain storm optimization algorithm, presented at 2019 IEEE Congress on Evolutionary Computation (CEC), Wellington, New Zealand, 2019, pp. 1044–1051.

[34] L. B. Ma, S. Cheng, and Y. H. Shi, Enhancing learning efficiency of brain storm optimization via orthogonal learning design, IEEE Trans. Syst. Man Cybernet. Syst., 2020, pp. 1–20.

[35] J. Cui, B. Hu, and S. Z. Chen, Resource allocation and location decision of a UAV-relay for reliable emergency indoor communication, *Comput. Commun.*, vol. 159, pp. 15–25, 2020.

[36] B. Yamauchi, Frontier-based exploration using multiple robots, in *Proc.* 2^{nd} *Int. Conf. Autonomous Agents*, New York, NY, USA, 1998, pp. 47–53.

Hui Lu received the PhD degree in navigation, guidance, and control from Harbin Engineering University, Harbin, China in 2004. She is a professor at Beihang University, Beijing, China. Her research interests include swarm optimization algorithm, fitness landscape analysis, and parameter control in combinatorial optimization problem, simulation, and scheduling technology in information and communication system.

Siyi Yang received the BS degree from Xiamen University, Xiamen, China in 2019. She is currently a master candidate at Beihang University. Her main research areas include communication and path planning in multi-robot system.

Shi Cheng received the bachelor degree in mechanical and electrical engineering from Xiamen University, Xiamen, China in 2005, the master degree in software engineering from Beihang University, Beijing, China in 2008, and the PhD degree in electrical engineering and electronics from the University of Liverpool, Liverpool, UK in 2013. He is an associate professor at the School of Computer Science, Shaanxi Normal University, Xi'an, China. His current research interests include swarm intelligence for optimization and learning techniques.

Meng Zhao received the BS degree from Communication University of China, Beijing, China in 2018. She is currently a doctoral student at Beihang University. Her main research areas include robot path planning and group intelligent navigation.